Polar Biol (2013) 36:1709–1722
DOI 10.1007/s00300-013-1388-3

ORIGINAL PAPER

Community structure and photosynthetic activity of benthic biofilms from a waterfall in the maritime Antarctica

Carlos Rochera · Eduardo Fernández-Valiente · Bart Van de Vijver · Eugenio Rico · Manuel Toro · Warwick F. Vincent · Antonio Quesada · Antonio Camacho

Received: 15 February 2013 / Revised: 1 July 2013 / Accepted: 9 August 2013 / Published online: 23 August 2013

Abstract High-energy flowing water habitats such as waterfalls are uncommon in Antarctica, though they may become more regular as temperature increase. Both high spatial and temporal environmental variability is expected on them. The extent of their biological colonization will depend on the amount of ecological strategies displayed by the surrounding biota. We report here a study on phototrophic microbenthic communities inhabiting such environment in a stream on the Byers Peninsula of Livingston Island. Five different biofilms were distinguished by colour, and were located in specific microhabitat types in the waterfall, which flowed down a steep canyon. Photosynthetic pigment content and microscopic observations demonstrated a different assemblage of chlorophytes, cyanobacteria and diatoms among them. Biofilms were not randomly distributed in the stream channel, which may be related to water flow, nutrient availability and moisture. The exopolymeric substances content, stoichiometry and pigment composition varied among biofilms, likely reflecting differences in the water and nutrients availability. The photosynthetic rates were in the range of the observed in previous studies in the site and varied according to the habitat within the stream. Communities dominated by chlorophytes were restricted to the central channel, suggesting adaptation to faster flow regime. However, cyanobacterial biofilms appeared in a great range of environmental conditions. They were rare in the central channel where water flow was greatest, but achieved large biomass stocks on submerged and even exposed sites in the splash zone at the edge of the flowing water. This study shows how Antarctic biofilms can have a large variability in community structure and biomass over short length scales, reflecting the range of microhabitats in this Antarctic waterfall ecosystem, and the potential occurrence of different strategies to overcome fluctuating conditions.

Keywords Byers Peninsula · Cyanobacteria · Diatoms · Exopolymeric substances · Inorganic carbon uptake · Stoichiometry

C. Rochera (✉) · A. Camacho
Departamento de Microbiología y Ecología, Instituto Cavanilles de Biodiversidad y Biología Evolutiva, Edificio de Investigación, Campus de Burjassot, Universitat de Valencia, 46100 Burjassot, Spain
e-mail: carlos.rochera@uv.es

E. Fernández-Valiente · A. Quesada
Departamento de Biología, Universidad Autónoma de Madrid, 28049 Madrid, Spain

B. Van de Vijver
Department of Bryophytes and Thallophytes, National Botanic Garden of Belgium, Domein van Bouchout, 1860 Meise, Belgium

E. Rico
Departamento de Ecología, Universidad Autónoma de Madrid, 28049 Madrid, Spain

M. Toro
Centro de Estudios Hidrográficos, CEDEX, 28005 Madrid, Spain

W. F. Vincent
Département de Biologie, Centre d'Études Nordiques, Université Laval, Sainte-Foy, QC G1K 7P4, Canada

Introduction

Phytobenthic populations are a common feature of streams at all latitudes, including Antarctica. In the McMurdo Dry Valleys, for example, thick films of cyanobacteria coat the bottom of seasonal streams, and persist throughout winter

in a freeze-dried state (Vincent and Howard-Williams 1986). Several studies have assessed the structure and function of these communities in ice-free areas of the continent (Broady 1982; Hawes 1989; Davey 1993; Vincent et al. 1993; Elster and Komarek 2003). However, few studies have explored them in cascades or waterfalls, given the rarity of these high-energy flowing water habitats in Antarctica. As a consequence of continuous climate warming in the polar regions, and notably in the maritime Antarctic region (Quayle et al. 2002; Vaughan et al. 2003), the occurrence of these waterfalls is likely to increase.

There are studies showing the wide occurrence of perennial photosynthetic microbial mats in Byers Peninsula (Fernández-Valiente et al. 2007; Velázquez et al. 2011; Rochera et al. 2013). But further observations have demonstrated also seasonal biofilms sparsely distributed in stream channels (Toro et al. 2007; Velázquez et al. 2011). These biofilms appear more dynamic than perennial microbial mats, which supposedly respond rapidly to changing environmental conditions (Velázquez et al. 2011). During snow melting and snow-free periods, lotic ecosystems from Antarctic ice-free areas are characterized by hydrodynamic fluctuations marked by highly variable water regimes (Inbar 1995). The discharge occurring during melting periods is thus responsive to climatic variations (Rochera et al. 2010). Under these circumstances, the fast-flow events disturb stream channels by removing sediments and abrading benthic biofilms. In contrast, after the completion of the ice melting, the flow regime decreases considerably and the habitat reconfigures with important changes in water and nutrient availability.

Bottom-up processes are thought to dominate river ecology. It is known that in the streams of temperate regions the development of benthic communities is regulated by disturbances such as the hydrological drought (Freeman et al. 1994; Caramujo et al. 2008) or nutrient availability (Guasch et al. 1995). Some of the studies mentioned above involve periods covering annual extremes over the course of a year. By contrast, Antarctic streams undergo major changes in shorter periods, which supposedly involve different successional and/or distributional patterns of the biota. The question is whether initial colonization processes occur after the ice melts or whether biofilms are mainly perennial forms with some capacity to recover from perturbations. Diverse biofilms with different adaptative strategies might therefore enhance the resilience of the entire ecosystem.

In the present study, we evaluated the composition and activity of photosynthetic biofilms inhabiting a stream in the Byers Peninsula region of Livingston Island, complementing previous studies on microbial mats in the area (Fernández-Valiente et al. 2007). Here, we present data on the distribution and photosynthetic activity of five different benthic communities along a cross-sectional transect. The study involved the characterization of the photosynthetic community assemblages, which comprises the quantification of their photosynthetic activities, the exopolymeric substances (EPS) and the isotopic signature and stoichiometric compositions of biofilms. We further investigated whether the occurrence of biofilms in this distinct ecosystem type is mediated by different environmental controls.

Materials and methods

Study site

The study was conducted during February 2002 in a stream sited in the southern beach of Byers Peninsula (Fig. 1; 62°34′35″–62°40′35″S/60°54′14″–61°13′07″W), a 60.6-km^2 ice-free area, located on the western end of Livingston Island (South Shetland Islands, Antarctica). The climate of the site is characterized by mean monthly summer temperatures ranging between 1 and 3 °C and an annual precipitation around 700 mm. In this region, the flow regime of streams is strongly dependent of summer thawing and therefore important fluctuations occur during the hydrological cycle. Further information about the limnology of the site is provided by Toro et al. (2007) and Rochera et al. (2010). The stream in which biofilms were growing is the discharge of a lake located on the central plateau of the Peninsula at 65 m a.s.l. (Fig. 1; Turbio Lake in Toro et al. 2007, unofficial name). Part of the stream runs through a pronounced slope. During the austral summer, the water discharge increases due to ice and snow melting. Maximum flows and water velocities in the streams of the region occur during this period, between December and January, with water velocities higher than 2.0 m s^{-1} and water flows over 0.9 m^3 s^{-1} (Toro et al. 2007). By contrast, lower flow regimes occur later during February, when maximum water velocities and flows in representative locations are 0.4 m s^{-1} and 0.04 m^3 s^{-1}, respectively. The studied stream in particular is characterized by a fast water flow during thaw periods that passes down a vertical drop of several metres (~20 m). This waterfall (Esmeralda Cascade, unofficial name) faces the south direction, and therefore, the hours of direct solar radiation during each day in summer are limited.

Sampling

The occurrence and relative dominance of biofilms in the Esmeralda Cascade (unofficial name) was surveyed along a transect of 5 metres at a resolution of 5 cm. This transect was chosen as representative of the transversal variations in flow across the waterfall. Observations were conducted

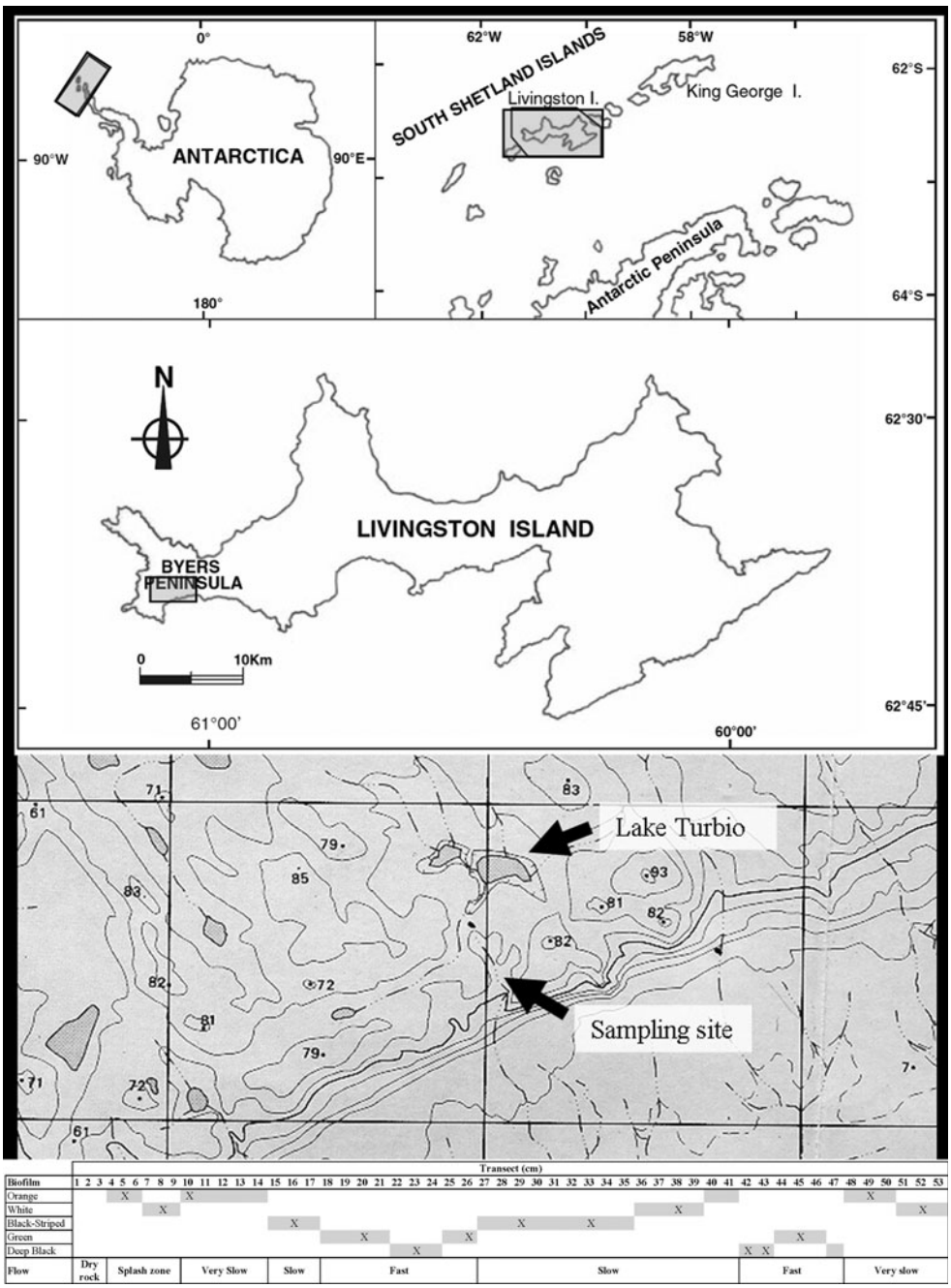

Fig. 1 Geographical location of Byers Peninsula (62°34′35″–62°40′35″S/60°54′14″–61°13′07″W) and distribution of biofilms in the studied site. The table below shows the distribution of biofilms along transect. Equis indicate the sites from samples were obtained

from the centre of the channel to the shore edge and to the sites that were splashed by water from the cascade. Once identified, samples of different biofilm types observed in the stream were randomly collected in triplicate from their representative locations (see Fig. 1) with a metal core taker (18 mm inner diameter). For the microscopical study, cores were placed in scintillation vials with formalin (4 % final concentration) and stored at +4 °C in the dark. Other cores were stored dry at −20 °C in sterile Whirlpak bags to perform the rest of the analyses.

Physical and chemical analysis of stream water

Conductivity and pH were measured using an YSI® 556 MPS Water Logger System. The samples for inorganic nutrients analysis were collected filtering the water trough precombusted glass-fibre filters (GF/F grade) and distributed in acid-cleaned polyethylene bottles. Subsequently they were frozen until they were processed in the laboratory following standard analytical methods (APHA 1992). Hence, ammonia (NH_4) was analysed by the phenol-

hypochlorite method. Nitrate plus nitrite (NO_x) was determined after reduction in nitrate to nitrite with cadmium coated with copper in a reduction column. Soluble reactive phosphorus (SRP) was assayed using ascorbic acid reduction in phosphomolybdate complex, and soluble reactive silica was measured by the molybdosilicate method. All the chemical measures were done in replicate. The concentrations of major ions (calcium, magnesium, sodium, potassium, sulphate and chloride) were determined with a Waters capillary ion analyzer. The bicarbonate concentration in water was measured calculating the alkalinity after titration with HCl using a pH shift indicator (phenolphthalein) of the equivalence end point pH. To measure the dissolved organic carbon (DOC), water samples were filtered through cellulose nitrate filters with a 0.2-μm pore size and dispensed in acid-cleaned glass bottles. They were stored at 4 °C until analysis. Once in the lab, DOC concentrations were determined by high-temperature oxidation with a Shimadzu TOC analyzer.

Phototrophic community structure and biomass

The taxonomic affiliation and relative abundances of the different phototrophs observed in biofilms were determined based on morphology. Cyanobacteria were identified following the classification system of Anagnostidis and Komarek (1988) and Komarek and Anagnostidis (1989). For microscopical analysis of diatoms, small quantities of the samples were cleaned by adding 37 % H_2O_2 to samples and posteriorly heated to 80 °C for 1 h. Oxidation of organic material was completed by the addition of $KMnO_4$. Following oxidation, the samples were rinsed 3 times with deionised H_2O and alternated with centrifugation (10 min at 3,700×*g*). The cleaned material was diluted with distilled water, dried on microscope cover slips and mounted in Naphrax mounting medium. Samples and slides are stored at the National Botanic Garden of Belgium (Meise, Belgium). In each sample, 400 valves were enumerated on random transects at 1,000× magnification under oil immersion using an Olympus BX51 microscope equipped with Differential Interference Contrast (Nomarski) optics. Identifications of Antarctic species are based on Kopalová et al. (2009), Sabbe et al. (2003), Van de Vijver (2008), Van de Vijver and Mataloni (2008), and Van de Vijver et al. (2010a, b; 2011).

To determine the distribution of photosynthetic pigments in the biofilms, chlorophylls and carotenoids were analysed by high-performance liquid chromatography (HPLC) using the methods described in Fernández-Valiente et al. (2007). Pigments were extracted from mats in pure acetone. Peak identities were determined by comparing retention times and spectra with those of pure standards purchased from DHI (Denmark). The amount of chlorophyll-a (Chl-a) in biofilms was used as an algal biomass indicator. Myxoxanthophyll, fucoxanthin and lutein were used as taxon-specific biomarkers for the determination of relative abundances of cyanobacteria, diatoms and chlorophytes, respectively. The ratio of absorbance at 480 and 665 nm of the extracts was used to describe the carotenoid content relative to Chl-a. This index was firstly described by Margalef (1960) and, in general, increase as algae are nutrient-limited. Variations of this ratio may also occur because of different light conditions. However, considering that all biofilms were subjected to the same light regime, we attribute differences observed merely to their nutritional/physiological condition. Dry weight of biofilms was determined on samples kept frozen after thawing and drying at 105 °C for 6 h.

To obtain the stoichiometric composition (carbon, nitrogen and phosphorus) of biofilms, carbon and nitrogen, contents were measured by the combustion of samples in a CE Instruments EA 1110 CHNS elemental analyzer. The samples were first dried at 60 °C until obtaining a stable weight. They were then ground to powder in a mortar, weighed over aluminium foil sleeves and burnt in the elemental analyzer. Gases released from burning were then measured by infrared analysis. The standard was prepared using sulphanilamide. Total phosphorus was obtained with the same method described for SRP after an acid digestion of the dried sample.

Determination of extracellular polymeric substances (EPS)

The amount of EPS in each biofilm was estimated as the total of their main components (carbohydrates and proteins). To extract these from biofilms, 1 ml of 2 % EDTA was added to around 10 mg of lyophilized sample, placed in Eppendorf® tubes, stirred and heated at 35 °C. After 1 h, these mixtures were centrifuged, and the supernatant was recovered for analysis. By following this procedure, we avoided to extract intracellular material. The carbohydrate content of extract was obtained by the measure of hexose equivalents in the supernatant using the phenol–sulphuric acid spectrophotometric method (Herbert et al. 1971) and using glucose as standard. The protein amounts were estimated from the same samples according to Bradford (1976), taking bovine serum albumin as a standard. All measurements were carried out on triplicate samples. For the microscopic observation of exo-carbohydrates distribution in biofilms, a portion of the 4 % formalin-fixed samples were dehydrated over glass slides and stained with Calcofluor White ($C_{40}H_{44}N_{12}O_{10}S_2$; λ excitation max = 347 nm and λ emission max = 436 nm) for 30 min. Preparations were observed through a Zeiss-III epifluorescence microscopy using the appropriate filter

setting for calcofluor fluorescence emission. Several pictures were taken with an Olympus® C-4040 ZOOM camera, and the RGB original images were converted into grayscale.

In situ ^{13}C-bicarbonate uptake in biofilms

The uptake of inorganic carbon in biofilms was measured by the stable isotopic method ($NaH^{13}CO_3$) described as follows. Experimental conditions were designed to discriminate photosynthetic from dark carbon assimilation. Thus, four cores (18 mm inner diameter) of each biofilm (3 light + 1 dark) were placed in sterile Whirl–pak® bags with 10 ml of filtered (GF/F) water from the site. The experiment was initiated by the addition of a volume of a concentrated solution of $H^{13}CO_3$ (99 % ^{13}C atoms) such that the proportion of isotope resulted in around 10 % of total dissolved organic carbon in water. Additional cores of each biofilm were incubated in parallel at the same conditions with formalin (4 % final concentration) to estimate passive carbon accumulation. All samples were incubated at ambient light intensity (measured with a Li-Cor® LI-193SA) and in situ temperature. Incubations were maintained for 2 h, and they were subsequently stopped by adding 3 ml of 1 N HCl. The bags were then opened to allow non-fixed carbon to escape as $^{13}CO_2$ gas. After neutralizing samples with NaOH 1 N, the water inside the bags was discarded. Cores were cleaned three times with Milli-Q grade water and then preserved in darkness at −20 °C. Once in the lab, the isotopic enrichment during uptake experiments of dry cores was measured in an IRMS Micromass-Isochrom mass spectrometer. The carbon assimilation rates were calculated as in Ariosa et al. (2006). The concentration of dissolved inorganic carbon in the incubation water (as needed for calculations) was determined from total alkalinity by pH. To establish comparisons among biofilms, uptake rates were normalized both to the surface and to Chl-*a* content.

Statistical analysis

Nonparametric Mann–Whitney tests were performed to evaluate differences in variables measured in distinct biofilms. Differences were considered significant when p value was less than 0.05. To identify major patterns of variability among biofilms, a principal component analysis (PCA) was conducted with a total of 15 variables measured in biofilms. Variables were log-transformed ($\log_{10} 1 + x$) to linearize the relationships and avoid the influence of magnitude. A categorical data matrix was created considering the relative abundance of different taxonomical groups in biofilms (i.e., absent = 0, present = 1, frequent = 2, abundant = 3). A hierarchic-agglomerative cluster analysis based on the UPGMA (unweighted pair group average linkage method) with the Euclidean Distance as a dissimilarity measure was performed (MVSP 3.13p, Kovach Computing Services 2002).

Results

Stream chemistry

The conductivity and inorganic nutrient concentrations in the waters flowing down the cascade were low (Table 1) and typical of oligotrophic polar streams. The molar ratio of dissolved combined nitrogen ($NO_3 + NO_2 + NH_4$) and SRP was around 15, implying a balanced supply for algal growth. The water was around neutral pH and DOC concentrations were low but above detection.

Distribution and physical features of biofilms

Different microphytobenthic communities coated the waterfall faces and the bed of the stream. Visual inspections made in situ showed the occurrence of five distinct biofilms with a monolayer structure. Based on macroscopic characteristics (surface colour, shade, roughness), different

Table 1 Main physical and chemical parameters of the stream water at February 2002

Parameter	Unit	Stream water
Temperature	°C	2.54
O_2	%	98.4
O_2	mg L^{-1}	13.4
Conductivity	μS cm^{-1}	68.00 (±9.67)
pH		7.22 (±0.11)
$NO_3 + NO_2$	μM	0.802 (±0.213)
NH_4	μM	0.856 (±0.276)
SRP	μM	0.116 (±0.012)
DIN/SRP	Molar ratio	14.3
Silicates	μM	46.91 (±12.31)
DOC	mg L^{-1}	0.6
DIC	mg L^{-1}	5.48
Cl^-	meq L^{-1}	0.26
SO_4^{2-}	meq L^{-1}	0.28
HCO_3^-	meq L^{-1}	0.65
K^+	meq L^{-1}	<0.05
Na^+	meq L^{-1}	0.57
Mg^{2+}	meq L^{-1}	0.22
Ca^{2+}	meq L^{-1}	0.49

For those parameters displaying a mean value (±standard deviation), it represents the average of three equidistant measures made along the area of biofilms distribution. In the other cases, the value represents a single measure made in the central part of the transect

names were assigned to each: *Deep Black*: DB; *Black-Striped*: BS; *Green*: GR; *White*: WH and *Orange*: OR. The biofilms showed a patchy distribution in a transect from the centre of the channel to the near-shore stream edge. Moisture varied partly relative to their location. The highest water content was observed in the *Green* biofilm (73 %), followed by *Black-Striped* (63 %), *Orange* (57 %), *Deep Black* (47 %) and *White* (40 %).

Both *Green* and *Deep Black* were the two biofilms showing the highest extension. The first was on average 2- to 3-mm thick (up to 4 mm) growing preferentially in running water with a dominant distribution in the centre of the stream basin. The *Deep Black* biofilm was thinner (1 mm) showing a more cohesive aspect compared to the former. This biofilm coated extensively the stream shores, where the water flow was lower. The rest of the biofilms grew wherever water flow decreased significantly. The *Black-Striped* biofilm prevailed in the sites where the bottom was continuously covered by a fine water layer. This biofilm was similar to *Deep Black* but with darker pigmentation and a thickness of around 0.5 mm. The *Orange* biofilm (2–3 mm thick) was restricted to splashing zones, receiving only intermittent surface moistening. Finally, the *White* biofilm (usually less than 1 mm thick) was associated with the sites where the water level was occasionally below the biofilm surface and the flow was nearly negligible. Unlike the other biofilms, this biofilm showed little cohesion and was dismantled easily. Microscopic examination of this biofilm revealed the occurrence of large numbers of nematodes, tardigrades and several ciliate morphotypes, however, a detailed study of the faunal components was not an objective for this study.

Community structure and photosynthetic activity

Algal biomass, expressed as chlorophyll-*a* (Chl-*a*) content per surface area, was significantly higher in the *Green* biofilm compared to the others (Table 2). Algal biomass was similar between *Deep Black*, *Black-Striped* and *Orange* biofilms, whereas *White* showed the lowest photosynthetic biomass. Besides chlorophyll, a diverse set of pigments was also detected with the HPLC analysis, including both pheophorbides and taxa-specific carotenoids. Pheophytin-*a*, a common degradation product of Chl-*a*, occurred in all biofilms, though its ratio to Chl-*a* was approximately 10-fold higher in the *White* biofilm compared to the others.

Myxoxanthophyll, the specific carotenoid of cyanobacteria, occurred in all communities except in the *Green* biofilm, although *Deep Black, Black-Striped* and *Orange* displayed higher relative contents of myxoxanthophyll. Lutein, particular of chlorophytes, was detected in the *Green*, *White* and *Black-Striped* biofilms although it was relatively higher in the *Green* compared to the *White* biofilm. In *Black-Striped* biofilms, lutein levels were low, and a possible co-elution with zeaxanthin might have resulted in an overestimation. Fucoxanthin, which occurs only in Bacillariophyceae, was observed in all extracts except in the *Orange* biofilm. This pigment was mostly found in the *White* and particularly in the *Green* biofilm communities; *Deep Black* showed the lowest levels of fucoxanthin. The total carotenoids/Chl-*a* ratios, estimated as the ratio between 480 and 665 nm in the acetone extracts, ranged from 0.61 to 1.74 (Table 2). Biofilms dominated by chlorophytes showed the lowest ratios, whereas the highest ratios were marginally observed in the *Orange* biofilm. On the other hand, ratios in *Deep Black* and *Black-Striped* biofilms were close to 1. UV-screening pigments such as scytonemin were not found in any of the investigated biofilms.

A list containing the main phototrophic micro-organisms inhabiting biofilms with their relative contribution is shown in Table 3. A cluster analysis based on these relative abundances (Fig. 2) allowed distinguishing the cyanobacterial-dominated biofilms (*Deep Black*, *Black-Striped* and *Orange*) from the other two (*Green* and *White*). In the former, the highest similarity was found between *Orange* and *Black Stripped*. To some extent, *Deep Black* thus represented a transition between both groups. The assemblages consisted principally of a variety of diatoms, green algae and cyanobacteria, with a total of 42 recognized taxa. Except in the *Green* and *White* biofilms, cyanobacteria were common in all communities on different levels. Four different filamentous morphotypes were found and tentatively assigned as *Oscillatoria* sp. 1 and *Oscillatoria* sp. 2 (5–6 and 9–10 μm width, respectively), *Phormidium* cf. *autumnale* (C.Agardh) Trevisan ex Gomont, and *Leptolyngbya* sp. In the *Black-Striped* biofilm, the phototrophic biomass consisted almost entirely of *Oscillatoria* sp1, accounting for 70–80 % of the total cyanobacterial biomass. *Oscillatoria* sp1 was also abundant in *Deep Black* but co-dominant with other morphotypes. *Oscillatoria* sp2 was less widespread, observed only in the *Black-Striped* and *Orange* biofilms. In the *Orange* biofilm, *Phormidium* cf. *autumnale* and *Leptolyngbya* sp. were present, but the latter was more abundant. *Phormidium* cf. *autumnale* prevailed more in *Deep Black* biofilm than in any other biofilms. In *White* biofilm, cyanobacterial morphotypes were scarce and only *Oscillatoria* sp1 was observed. *Ulothrix* sp. was the most dominant chlorophycean in *Green* and *White* biofilms. Of all the cyanobacterial biofilms, this green alga only occurred in the *Deep Black*. The relative abundances of small flagellates, assigned to the Chrysophycean genera *Ochromonas*, also varied among biofilms, being more abundant in *Green* and, to a lesser extent, in *White*. They sometimes constituted less than 1 % of biomass in cyanobacterial-dominated biofilms, being more abundant in the *Deep Black*.

Table 2 Pigment composition expressed as ratios to chlorophyll-*a* (wt/wt) in the different biofilms obtained by means of HPLC analysis with purified pigments as standards (DHI, Denmark)

Biofilm	Chlorophyll-*a*	Phaeophytin-*a*	Fucoxanthin	Myxoxanthophyll	Lutein	Car/Chl-*a* ratio
Green	48.14	0.069	0.364	n.d.	0.174	0.70
Deep black	25.76	0.023	0.017	0.229	n.d.	1.07
Black-striped	25.82	0.314	0.109	0.061	0.108	1.19
Orange	24.45	0.045	n.d.	1.230	n.d.	1.74
White	9.07	1.124	0.188	0.018	0.146	0.61

Chlorophyll-*a* is expressed as μg $(cm)^{-2}$ and phaeophytin-*a*, fucoxanthin, myxoxanthophyll and lutein as μg (μg chlorophyll-*a*)$^{-1}$

n.d. not detected

A total of 37 diatom taxa were retrieved by microscopical inspection. They were numerically the most abundant component in *White* biofilm and, to a lesser extent, present in *Green* and *Black-Striped*. Their contribution in the *Orange* biofilm was minor. The cosmopolitan *Fragilaria capucina* s.l. Desm. was the principal species in diatom-dominated assemblages. Other diatoms showed a less cosmopolitan distribution. For example, species such as *Gomphonema signyensis* V.J. Jones & Kociolek, *Nitzschia frustulum* (Kütz.) Grunow and *Psammothidium metakryophilum* (Schmidt & Lange-Bert.) Sabbe were only observed in *Green* and *White* biofilms. Other species such as *Staurosirella pinnata* (Ehrenb.) D.M.Williams & Round, *Nitzschia acidoclinata* Lange-Bert., *Navicula cremeri* Van de Vijver were, by contrast, only observed in *Deep Black* biofilm. In the *White* biofilm, we observed some aerophilic diatoms such as *Hantzschia hyperaustralis* Van de Vijver & Zidarova, *Muelleria australoatlantica* Van de Vijver & Spaulding, *Luticola cohnii* (Hilse) D.G. Mann and *Diadesmis arcuata* (Heiden) Lange-Bert., although their relative abundances were lower compared to other taxa.

The areal rates of inorganic carbon uptake differed significantly among the biofilms under the conditions assayed (Fig. 3). The highest rates were observed in *Deep Black*, although they were not significantly different to those displayed by *Green* and *Black-Striped* biofilms. In contrast, significantly, lower rates were measured in *Orange* and *White* compared to the other biofilms. No significant differences were observed for the carbon assimilation in the dark treatments versus the formalin-fixed controls, indicating thus that all carbon assimilation measured in the experiment was performed by photosynthetic organisms.

Biomass and stoichiometric composition of biofilms

The bulk biomass elemental composition (carbon, nitrogen and phosphorus) of the biofilms and their stoichiometric relationships are shown in Table 4. Values ranged across approximately one order of magnitude, with the minimum and maximum mean values as follows: 255.2 and 38.8 mg g dw^{-1} for carbon, 36.9 and 3.9 mg g dw^{-1} for nitrogen and 5.2 and 1.0 mg g dw^{-1} for phosphorus, respectively. *Green* displayed the highest and *White* the lowest concentrations of the three nutrients. In biofilms dominated by cyanobacteria, *Deep Black* and *Black-Striped* showed similar values for the three nutrients, but values were lower in *Orange*. The three elements co-varied in the biofilms, and molar ratios did not differ notably among them. Only the *Orange* community showed certain phosphorus deficiency with respect to the carbon content. This biofilm also showed the highest C/N relationship. Both C/N and N/P molar ratios varied in a similar degree, ranging from 7.2 to 17.1 and from 9.0 to 17.7, respectively. The C/P ratio showed the widest variation among biofilms, with high and low values of 106.4–211.4, respectively. Some differences were observed concerning the ^{13}C natural abundances among the biofilms (Table 4). The lower delta values of −21.3 ‰ and −16.1 ‰ occurred in the *Green* and *White* biofilms, respectively, while relatively enriched delta values of −14.5, −13.3 and −11.7 ‰ were observed in the *Orange*, *Deep Black* and *Black-Striped* biofilms, respectively.

Exopolymeric substances (EPS) distribution in biofilms

The heterogeneity observed among biofilms was also reflected in their EPS (Fig. 4a). Significantly, higher amounts of EPS per dry weight were observed in *Deep Black* biofilms, whereas *Green*, *Black-Striped* and *Orange* biofilms all had similar values. The *White* biofilms showed significantly lower values. Weight ratios for EPS carbohydrate and protein content also varied notably (Fig. 4b). A significantly higher proportion of carbohydrates relative to proteins was observed in *Orange*. This ratio was also significantly higher in *White* biofilm with respect to the *Green*, *Deep Black* and *Black-Striped* biofilms, which showed lower ratios. Since the EDTA-extractable carbohydrates comprise the EPS matrix of biofilms (colloidal fraction) as well as the sheaths of micro-organisms (capsular fraction), these values represent the sum of both. Using the calcofluor white probe, a stain for carbohydrates,

Table 3 Relative abundances of different phototrophic microorganisms inhabiting the five biofilms, indicated as follows: +, present; ++, frequent; +++, abundant; –, absent

Taxa	Green	Deep black	Black-striped	Orange	White
Cyanobacteria					
Oscillatoria sp1. (5–6 μm width)	+	++	+++	++	+
Oscillatoria sp2. (9–10 μm width)	–	–	+	+	–
Phormidium cf. *autumnale*	–	++	–	+	–
Leptolyngbya sp.	–	++	+	+++	–
Bacillariophyceae					
Amphora veneta	–	–	–	–	+
Brachysira minor	–	–	–	+	–
Caloneis bacillum	–	–	–	–	+
Chamaepinnularia gerlachei	++	–	+	+	–
Chamaepinnularia krookiiformis	–	–	–	+	+
Diadesmis arcuata	–	–	–	–	+
Diadesmis comperei	–	+	–	+	+
Eolimna jamesrossensis	–	+	–	–	+
Fragilaria capucina s.l.	+++	+++	++	+++	++
Gomphonema signyensis	–	–	+	–	+
Gomphonema sp.	–	+	–	++	++
Hantzschia amphioxys	–	–	+	–	–
Hantzschia hyperaustralis	–	–	–	–	+
Hippodonta hungarica	–	–	+	–	+
Luticola australoatlantica	–	–	+	+	–
Luticola cohnii	–	–	–	–	+
Muelleria australoatlantica	–	–	–	–	+
Navicula australoshetlandica	–	–	–	+	+
Navicula cremeri	–	+	–	–	–
Navicula gregaria	–	–	–	–	+
Nitzschia acidoclinata	–	+	–	–	–
Nitzschia cf. gracilis	+++	++	+	+	++
Nitzschia frustulum	–	+	+	–	+
Nitzschia homburgiensis	–	–	+	–	+
Nitzschia inconspicua	++	–	–	+	+
Nitzschia paleacea	–	–	+	+	+
Nitzschia perminuta	+	–	–	+	+
Pinnularia borealis scalaris	–	–	–	–	+
Pinnularia microstauron	+	+	–	–	+
Pinnularia subantarctica elongata	–	–	–	–	+
Planothidium delicatulum	–	+	–	+	+
Planothidium frequentissimum	–	–	–	+	+
Planothidium haynaldii	–	–	+	–	–
Planothidium lanceolatum	–	–	+	–	+
Psammothidium metakryophilum	–	–	+	+	+
Sellaphora nana	–	+	–	–	+
Staurosirella pinnata	–	+	–	–	–
Green algae					
Ulothrix sp.	+++	+	–	–	+++
Chrysophyceae					
Ochromonas-like	+++	++	–	+	+++

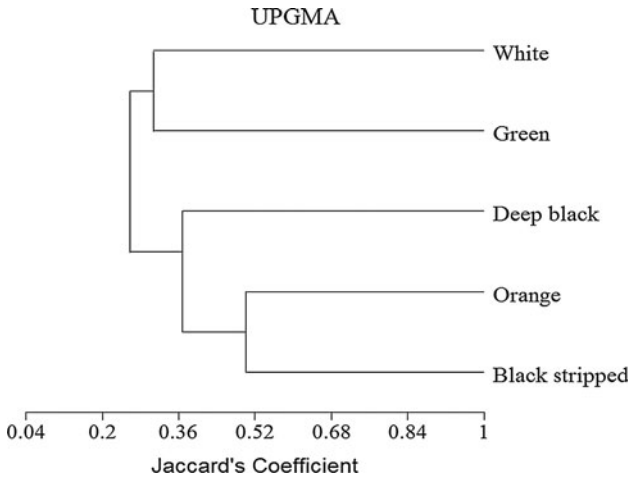

Fig. 2 Biofilms cluster of UPGMA linkage using the Euclidean distance. Mainly, the analysis revealed two major groups based on algae assemblages: (1) *White* and *Green* and (2) *Orange* and *Black Stripped*. *Deep Black* likely represents a transient assemblage among them

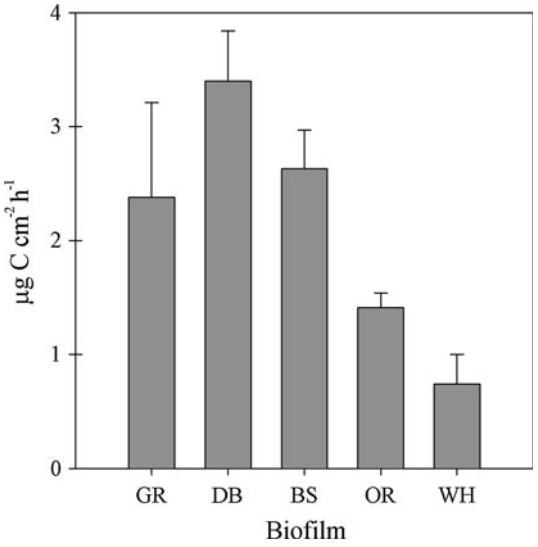

Fig. 3 Areal photosynthetic rates of inorganic carbon assimilation measured in the five biofilms. *Green* (GR), *Deep Black* (DB), *Black-Striped* (BS), *Orange* (OR) and *White* (WH). Uptake rates were obtained by subtracting values obtained at dark conditions to those obtained under illuminated conditions. The average photosynthetic active radiation (PAR) light during incubations was 250 µ mol photons m^{-2} s^{-1}

we identified the fraction of EPS associated with cyanobacterial sheaths (Fig. 5), confirming that this fraction differs among the cyanobacterial morphotypes. *Oscillatoria* sp1, which was abundant in cyanobacterial-dominated biofilms, was positively stained with calcofluor. It was characterized by a thick polysaccharide layer of carbohydrate inclusions (Fig. 5b), likely composed of glycogen. As shown in Fig. 5a, a large number of diatoms were attached to the trrichomes of this cyanobacterium. The *Leptolyngbya* dominating in the *Orange* biofilm also showed an EPS-rich sheath (Fig. 5c), whereas *Oscillatoria* sp2 had a more discrete layer of polysaccharides deposited outside the cell (Fig. 5d). By contrast, the *Phormidium* cf. *autumnale* observed in this same biofilm lack fluorescent signals when excited (Fig. 5b).

Multivariate analysis

PCA was performed to test the weight of different factors explaining the variability observed between biofilms (Fig. 6). Components 1 and 2 comprised 79.59 % of total variance. Component 1 accounted for 54.91 % of variability and was strongly associated with biofilms stoichiometry and photosynthetic activity. The ratio between carotenoids and chlorophylls (ratio 480/665 nm) had by contrast a lower weight, as indicated by the small range of the axis score for this variable. In this axis, the *White* biofilm was clearly separated from the rest on the negative side, indicating a close relationship with degradation products and lower photosynthetic activity and nutrients content. On the other hand, component 2 accounted for 24.67 % of variability. In this axis, myxoxanthophyll and $\partial^{13}C$ had higher positive weights, whereas fucoxanthin had the highest negative loading, demonstrating a close relation between this component and the taxonomic composition of biofilms. Accordingly, biofilms dominated by cyanobacteria (*Deep Black*, *Orange* and *Black-Striped*) were located on the positive side, while *Green* was on the negative side.

Discussion

Our findings demonstrate a heterogeneous distribution of biofilm types over the riverbed, with distinct communities occurring in the waterfall. The main structural factor behind the observed spatial heterogeneity of biofilms in Esmeralda Cascade appears to be the selective stresses exerted by the water regime. As observed in other Antarctic streams, strong currents can limit periphyton growth by scraping and lifting off algal biomass from the stream substrate (Elster and Komarek 2003 and articles cited therein). This occurs often when running water contains an elevated load of suspended particles. The central stream channel was densely overgrown by a biofilm dominated by filamentous chlorophytes, whereas those situated in the margins and rivulets, and especially those isolated from continuous water flow, showed assemblages that ranged from a clear dominance of cyanobacteria to those with abundant diatoms. The development of cyanobacteria in the centre of the channel thus appears excluded by the faster current, favouring biofilms composed of chlorophytes that can thrive in more turbulent conditions.

Table 4 Elemental composition (carbon, nitrogen and phosphorus) of bulk biomass and the natural isotopic abundance of ^{13}C in the five biofilms studied

Parameter	Unities	Green	Deep black	Black-striped	Orange	White
C	mgr g dw^{-1}	255.21 ± 51.49	187.70 ± 50.35	208.76 ± 17.76	187.54 ± 25.37	38.84 ± 4.47
N	mgr g dw^{-1}	36.94 ± 5.57	30.07 ± 6.47	27.28 ± 0.39	12.82 ± 1.87	3.87 ± 0.04
P	mgr g dw^{-1}	5.20 ± 0.34	4.49 ± 0.02	3.42 ± 0.20	2.36 ± 0.41	0.99 ± 0.25
C/N	Molar ratio	8.03 ± 0.42	7.24 ± 0.40	8.92 ± 0.63	17.08 ± 0.18	11.70 ± 1.23
N/P	Molar ratio	15.85 ± 3.40	14.82 ± 3.25	17.68 ± 1.27	12.40 ± 3.94	8.97 ± 2.33
C/P	Molar ratio	127.94 ± 33.91	107.95 ± 29.43	158.15 ± 22.49	211.40 ± 65.01	106.38 ± 38.28
$\delta^{13}C$	‰	−21.30	−13.30	−11.70	−14.50	−16.10

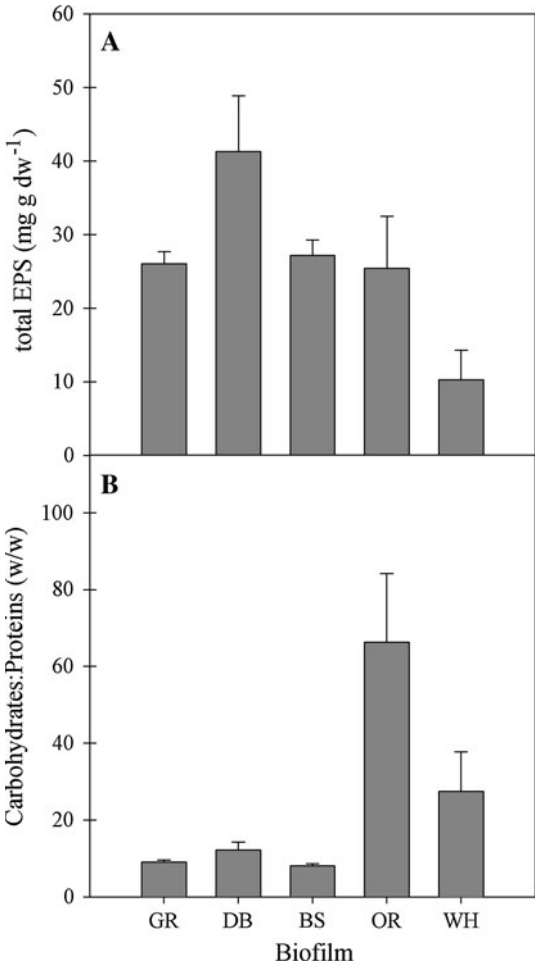

Fig. 4 Distribution of exopolymeric substances (EPS) in the biofilms. **a** Total amounts of EDTA-extractable EPS in biofilms. **b** Weight ratios of carbohydrates versus proteins in EPS extracted from biofilms

The dominant micro-organisms observed in these biofilms are common in cold environments. For instance, *Phormidium* cf. *autumnale* has been reported in biogeographical studies as frequently observed taxa in Antarctic biotopes (Taton et al. 2003). The dominant diatom species, *Fragilaria capucina*, is a common constituent of rivers and brooks on several sub-Antarctic islands, forming often populations of more than 90 % of all diatoms present in the rivers (Van de Vijver and Beyens 1999). The genus is known for its ability to bloom opportunistically, with elevated growth rates and a rapid colonization capability (Denys 1990; Lotter and Bigler 2000), features that imply adaptation to dynamic environments such as the stream in this study. Although the amount of aerophilic diatoms was too low to indicate that biofilms dry out completely, they were more common in biofilms subjected to more dryness.

Carbon fixation rates measured in the more active biofilms are comparable to those observed in other localities of the maritime Antarctic region such as King George Island (3.0–3.6 μg C cm^{-2} h^{-1}; Hawes 1989). On the other hand, values obtained for the *Orange* and *White* biofilms fall in the range were observed for cyanobacterial communities in the McMurdo Dry Valleys (0.39–2.15 μg C cm^{-2} h^{-1}; Vincent and Howard-Williams 1986). In our case, biofilms subjected to high water flow showed higher photosynthetic rates, suggesting that productivity and water current may be coupled. Different nutrient uptakes can occur due to differences in the water flow velocity (Simon et al. 2004), which can be related with certain functional aspects of biofilms. As Morris and Monier (2003) noted, biofilms tend to have rough surfaces under turbulence or shearing stress, involving a reduction in boundary layer thickness. This produces a facilitation of mass transfer from water to the biofilm, which translates in a higher carrying capacity for the biofilms under high stream velocity. This may explain the higher productivity of biofilms located in the centre of the stream. In other respects, developing of rough surfaces might also explain the formation of streamers observed in the surface of some of the biofilms.

As mentioned before, both *Orange* and *White* biofilms showed lower areal photosynthetic activity compared to other biofilms. However, for specific photosynthetic activity (i.e., values normalized to Chl-*a* content), *Orange* displayed the highest photosynthetic yield. This difference in the photosynthetic rates (areal vs. specific), which was also observed in microbial mats from the same site

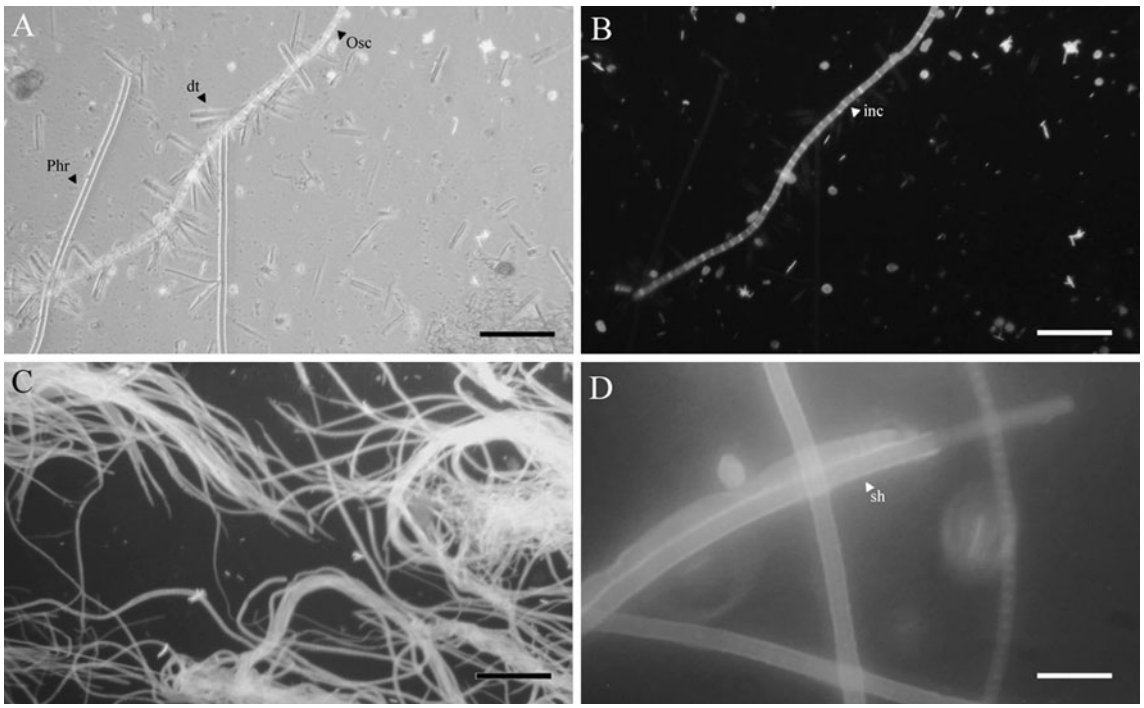

Fig. 5 Visible light and epifluorescent microscopy photographs of biofilms stained with Calcofluor White dye showing common cyanobacterial morphotypes found in the biofilms of Peninsula Byers. **a** Visible light picture from biofilm showing *Phormidium* (Phr) and *Oscillatoria* sp1 (Osc) filaments attached by numerous diatoms (dt). **b** Epifluorescence image from same field showing only *Oscillatoria* filament and the presence of carbohydrate inclusions (inc) in cells. **c** Epifluorescence pictures of *Leptolyngbya* from *Orange* biofilm showing EPS-rich glycocalyx sheath (sht). **d** *Oscillatoria* sp2 from *Orange* biofilm showing a polysaccharides layer deposited outside the cells. *Bar* indicates 50 μm in all cases

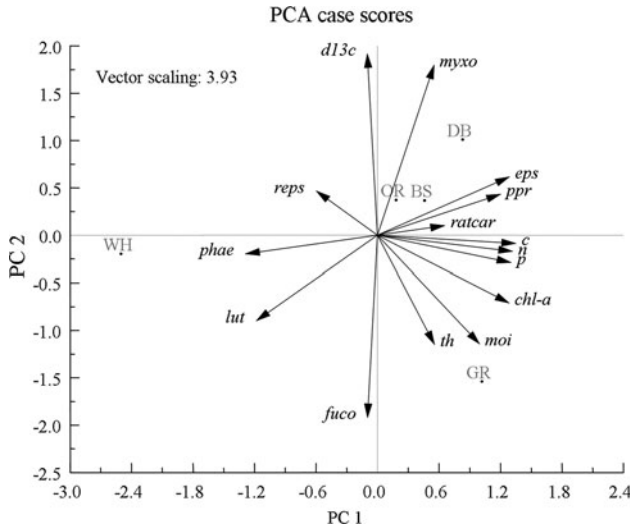

Fig. 6 Distribution of biofilms and measured variables plotted by 1st and 2nd components of PCA analysis. Labels are: th: biofilm thickness; c: carbon; n: nitrogen p: phosphorus; eps: total EPS reps: ratio carbohydrates versus proteins in EPS; moi: biofilm moisture; chl-a: chlorophyll-*a* per surface; ratcar: ratio 480/665 nm; d13c: $\partial^{13}C$ in biofilm; ppr: photosynthetic rates; phae: phaeophytin-*a*; fuco: fucoxanthin; myxo: myxoxanthophyll; lut: lutein

(Fernández-Valiente et al. 2007), indicates that the phototrophic community of this biofilm is devised to maintain low growth rates, which furthermore could be indicating that is well-adapted to thrive under low nutrient conditions. There were additional parallels between the present biofilms and the microbial mats studied by Fernández-Valiente and co-workers. Thus, higher and comparable photosynthetic rates are observed in the microbial mat located in the stream and in the biofilms less affected by water availability (*Deep Black*, *Green* and *Black-Striped*). On the contrary, the microbial mats from soils and ponds displayed similar photosynthetic rates to the *Orange* biofilm, and all were characterized by a higher drought stress.

Our findings suggest a trade-off between water current (i.e., water renewal) and nutrient availability. Presumably, biofilms establish in the riverbed in the short time period just after thawing, just when the water discharge on the drainage channels are highest. When the present study was carried out (February), flow was low and therefore, stresses associated with full-flowing events were partially relieved, even though stresses related to low nutrient renewal should be high at this time. Our results are consistent with a study

elsewhere on Livingston Island that focused on carbon and nitrogen dynamics in two stream benthic communities (Davey 1993). In that study, although the author proposed that algal biofilms were not limited by nutrient availability, evoking instead a major role for other physical factors (irradiance and temperature), he found that atomic ratios (N/P) were more balanced in the mat inhabiting the central channel (dominated by chlorophytes) compared to mats on the margins (dominated by cyanobacteria). Our results support those observed along a gradient of water availability by Elster (2002). This author stated that in polar environments filamentous cyanobacteria dominate habitats with reduced water availability, probably related to the ability to recover from freezing and/or desiccation.

Although EPS production can also be ascribed to other microbial components of biofilms like diatoms (de Brouwer and Stal 2002; Chiovitti et al. 2003), bacteria or chlorophytes (Kroen and Rayburn 1984, Paulsen and Vieira 1994), in our case, their occurrence seems related to adaptive strategies involving cyanobacteria. For instance, EPS are known to offer adaptive features for coping with dryness. In this sense, the moisture content of the *Orange* biofilm is greater than expected due to its stream location. The EPS matrix provides a constant degree of moisture inside the biofilms, which might explain why this biofilm was even wetter than *Deep Black* biofilm. EPS likely has additional physiological functions. Unlike the other biofilms, whose molar ratios did not show a notable nutritional unbalance, *Orange* biofilm had a clear phosphorus deficiency with respect to its carbon content, as well as a higher C/N ratio. As noted before, this nutritional unbalance might be due to limited nutrient renewal as a consequence of limited water availability. This nutrient deficiency could also explain the higher relative content of carbohydrates compared to protein in the EPS composition, since carbohydrates have a much higher content of carbon relative to nitrogen or phosphorus compared to proteins. In addition, although this biofilm does not contain the highest amounts of EPS per dry weight, it has a high EPS content relative to the photosynthetically fixed carbon, meaning a substantial fraction is assigned to the production of carbohydrate-rich EPS. It is plausible since neither nitrogen nor phosphorus, both limited in this biofilm, are incorporated into carbohydrates. Whereas growth is limited when nutrients are in short supply, cells go on taking up carbon, and therefore primary production progresses at all times. This is a physiological strategy that allows cyanobacteria to keep a balanced elemental composition in cells while driving out secondary metabolites with an elevated carbon quota. This mechanism was reported by Otero and Vincenzini (2004) in experiments showing how EPS production in a cyanobacterial strain of the genera *Nostoc* worked like a carbon sink when the C/N relationship in the media was high. The high content of EPS relative to biomass might also allow the biofilm to cope with moisture stress, as suggested above. The occurrence of cyanobacterial species with carbohydrate-rich sheaths in the *Orange* biofilm, as demonstrated by staining with calcofluor white (Fig. 5), indicates that carbohydrate accumulation must occur primarily in the mucilaginous sheath of biofilm cyanobacteria (both *Leptolyngbya* and *Oscillatoria*). Differences observed in the $\partial^{13}C$ signatures could be also related with the production of EPS, since carbohydrates tend to become more enriched with the heavy isotope (Van Dongen et al. 2002).

Unlike biofilms dominated by cyanobacteria, those formed by green algae cannot overcome stress factors beyond their range of distribution and thus react differently to desiccation. For example, higher numbers of protozoa and invertebrate fauna in the *White* biofilms (personal observation) indicate significant invertebrate bioturbation. The role of EPS as a cyanobacterial defensive strategy against protozoa grazing has been previously reported (Pajdak-Stós et al. 2001). Since sheathed cyanobacteria are scarce in the *White* biofilms, this biofilm is likely more disposed to grazing. This idea is also supported by the high phaeophytin-*a*/Chl-*a* ratio of this biofilm compared to the other biofilms, indicating a higher algal detritus (Camacho and de Witt 2003). This biofilm is likely in a senescence state, as seen in highly productive green algae biofilms experiencing progressive degradation when non-autotrophic biological activities prevail. It might correspond to a more extended distribution of this algal assemblage during ice melting, when stream flow was higher and water covered more of the basin surface. This contrasted with the perennial character of the slow-growing cyanobacterial biofilms, which cannot grow under fast-flow conditions. In summary, our results imply that there are large differences on ecological strategies among different biofilm types, giving rise to a heterogeneous distribution of communities within the Esmeralda waterfall ecosystem.

Acknowledgments Fieldwork was supported by grant REN2000-0435-ANT from the Science and Technology Ministry (Spain) to AQ. Sample processing was supported by grant CGL2005-06549-C02-02/ANT from the Spanish Ministry of Education and Science to AC, which was co-financed by European FEDER funds. We are very thankful to the UTM (Maritime Technology Unit, CSIC) and Las Palmas crew (Spanish Navy) who provided us with the logistical support to make possible this expedition. We also acknowledge the constructive comments of the reviewers.

References

Anagnostidis K, Komarek J (1988) Modern approach to the classification system of cyanophytes. 3-Oscillatoriales. Arch Hydrobiol Suppl Algol Stud 50–53:327–472

APHA-AWWA-WPCF (1992) Standard methods for the examination of water and wastewater, 18th edn. American Public Health Association, Washington, DC

Ariosa Y, Carrasco D, Quesada A, Fernández-Valiente E (2006) Incorporation of different N sources and light response curves of nitrogenase and photosynthesis by cyanobacterial blooms from rice fields. Microb Ecol 51:394–403

Bradford MM (1976) A rapid and sensitive method for the quantification of microgram quantities of protein utilizing the principle of protein dye binding. Anal Biochem 72:248–259

Broady PA (1982) Taxonomy and ecology of algae in a freshwater stream in Taylor Valley, Victoria Land, Antarctica. Arch Hydrobiol Suppl Algol Stud 32:331–349

Camacho A, de Witt R (2003) Effect of nitrogen and phosphorus additions on a benthic microbial mat from a hypersaline lake. Aquat Microb Ecol 32:261–273

Caramujo MJ, Mendes CRB, Cartaxana P, Brotas V, Boavida MJ (2008) Influence of drought on algal biofilms and meiofaunal assemblages of temperate reservoirs and rivers. Hydrobiologia 598:77–94

Chiovitti A, Higgins MJ, Harper RE, Wetherbee R (2003) The complex polysaccharides of the raphid diatom *Pinnularia viridis* (Bacillariophyceae). J Phycol 39:543–554

Davey MC (1993) Carbon and nitrogen dynamics in a maritime Antarctic stream. Freshwater Biol 30:319–330

De Brouwer JFC, Stal LJ (2002) Daily fluctuations of exopolymers in cultures of the benthic diatoms *Cylindrotheca closterium* and *Nitzschia* sp. (Bacillariophyceae). J Phycol 38:464–472

Denys L (1990) *Fragilaria* blooms in the Holocene of the western coastal plains of Belgia. In: Simola H (ed) Proceedings of the tenth international diatom symposium, Joensuu, Finland, 28th August-2nd September 1988. Koeltz Scientific Books, Koenigstein, pp 397–406

Elster J (2002) Ecological classification of terrestrial algal communities in polar environments. In: Beyer L, Bölter M (eds) Geoecology of Antarctic ice-free coastal landscapes. Springer, Berlin, pp 303–326

Elster J, Komarek O (2003) Ecology of periphyton in a meltwater stream ecosystem in the maritime Antarctic. Antarct Sci 15:189–201

Fernández-Valiente E, Camacho A, Rochera C, Rico E, Vincent WF, Quesada A (2007) Community structure and physiological characterization of microbial mats in Byers Peninsula, Livingston Island (South Shetland Islands, Antarctica). FEMS Microbiol Ecol 59:377–385

Freeman C, Gresswell R, Guasch H, Hudson J, Lock MA, Reynolds B, Sabater F, Sabater S (1994) The role of drought in the impact of climatic change on the microbiota of peatland streams. Freshwater Biol 32:223–230

Guasch H, Martí E, Sabater S (1995) Nutrient enrichment effects on biofilm metabolism in a Mediterranean stream. Freshwater Biol 33:373–383

Hawes I (1989) Filamentous green algae in freshwater streams on Signy Island, Antarctica. Hydrobiologia 172:1–18

Herbert D, Phipps PJ, Strange RE (1971) Chemical analysis of microbial cells. In: Norris JR, Ribbons DW (eds) Methods in microbiology, vol 5B. Academic Press, London, pp 209–344

Inbar M (1995) Fluvial morphology and streamflow on Deception Island, Antarctica. Papers from symposium: Arctic and Alpine geomorphology and environmental change, Geografiska Annaler, series A. Phys Geogr 77:221–230

Komarek J, Anagnostidis K (1989) Modern approach to the classification system of cyanophytes. 4-Nostocales. Arch Hydrobiol Suppl Algol Stud 56:247–345

Kopalová K, Elster J, Nedbalová L, Van de Vijver B (2009) Three new terrestrial diatom species from seepage areas on James Ross Island (Antarctic Peninsula Region). Diatom Res 24:113–122

Kroen WK, Rayburn WR (1984) Influence of growth status and nutrients on extracellular polysaccharide synthesis by the soil alga *Chlamydomonas mexicana* (Chlorophyceae). J Phycol 20:253–257

Lotter AF, Bigler C (2000) Do diatoms in the Swiss Alps reflect the length of ice-cover? Aquat Sci 62:125–141

Margalef R (1960) Valeur indicatrice de la composition des pigments du phytoplankton sur la productivité, composition taxinomique et propiétés dynamiques des populations. Rapp Proc Verbo CIESM 15:277–281

Morris CE, Monier JM (2003) The ecological significance of biofilm formation by plant-associated bacteria. Annu Rev Phytopathol 41:429–453

Otero A, Vincenzini M (2004) *Nostoc* (Cyanophyceae) goes nude: extracellular polysaccharides serve as a sink for reducing power under unbalanced C/N metabolism. J Phycol 40:74–81

Pajdak-Stós A, Fialkowska E, Fyda J (2001) *Phormidium autumnale* (Cyanobacteria) defense against three ciliate grazer species. Aquat Microb Ecol 23:237–244

Paulsen BS, Vieira AAH (1994) Structure of the capsular and extracellular polysaccharides produced by the desmid *Spondylosium panduriforme* (Chlorophyta). J Phycol 30:638–641

Quayle WC, Peck LS, Peat H, Ellis-Evans JC, Harrigan PR (2002) Extreme responses to climate change in Antarctic lakes. Science 295:645

Rochera C, Justel A, Fernández-Valiente E, Bañón M, Rico E, Toro M, Camacho A, Quesada A (2010) Interannual meteorological variability and its effects on a lake from maritime Antarctica. Polar Biol 33:1615–1628

Rochera C, Villaescusa JA, Velázquez D, Fernández-Valiente E, Quesada A, Camacho A (2013) Vertical structure of bi-layered microbial mats from Byers Peninsula, Maritime Antarctica. Antarct Sci 25:270–276

Sabbe K, Verleyen E, Hodgson DA, Vanhoutte K, Vyverman W (2003) Benthic diatom flora of freshwater and saline lakes in the Larsemann Hills and Rauer Islands, East-Antarctica. Antarct Sci 15:227–248

Simon KS, Townsend CR, Biggs BJF, Bowden WB (2004) Temporal variation of N and P uptake in 2 New Zealand streams. JN Am Benthol Soc 24:1–18

Taton A, Grubisic S, Brambilla E, de Wit R, Wilmotte A (2003) Cyanobacterial diversity in natural and artificial microbial mats of Lake Fryxell (McMurdo Dry Valleys, Antarctica): a morphological and molecular approach. Appl Environ Microbiol 69:5157–5169

Toro M, Camacho A, Rochera C, Rico E, Bañón M, Fernández-Valiente E, Marco E, Justel A, Vincent WF, Avendaño MC, Ariosa Y, Quesada A (2007) Limnological characteristics of freshwater ecosystems of Byers Peninsula, Livingston Island (South Shetland Islands, Antarctica). Polar Biol 30:635–649

Van de Vijver B (2008) *Pinnularia obaesa* sp. nov. and *P. australorabenhorstii* sp. nov., two new large *Pinnularia* (sect. Distantes) from the Antarctic King George Island (South Shetland Islands). Diatom Res 22:221–232

Van de Vijver B, Beyens L (1999) Freshwater diatoms from Ile de la Possession (Crozet Archipelago, Subantarctica): an ecological assessment. Polar Biol 22:178–188

Van de Vijver B, Mataloni G (2008) New and interesting species in the genus *Luticola* D.G. Mann (Bacillariophyta) from Deception Island (South Shetland Islands). Phycologia 47:451–467

Van de Vijver B, Mataloni G, Stanish L, Spaulding S (2010a) New and interesting species of the genus *Muelleria* (Bacillariophyta) from the Antarctic Region and South Africa. Phycologia 49:22–41

Van de Vijver B, Sterken M, Vyverman W, Mataloni G, Nedbalova L, Kopalova K, Elster J, Verleyen E, Sabbe K (2010b) Four new

non-marine diatom taxa from the Subantarctic and Antarctic Regions. Diatom Res 25:431–443

Van de Vijver B, Zidarova R, Sterken M, Verleyen E, de Haan M, Vyverman W, Hinz F, Sabbe K (2011) Revision of the genus *Navicula* s.s. (Bacillariophyceae) in inland waters of the Sub-Antarctic and Antarctic with the description of five new species. Phycologia 50:281–297

van Dongen BE, Schouten S, Sinninghe Damsté JS (2002) Carbon isotopic variability in algal and terrestrial carbohydrates. Mar Ecol Prog Ser 232:83–92

Vaughan DG, Marshall G, Connolley WM, Parkinson C, Mulvaney R, Hodgson DA, King JC, Pudsey CJ, Turner J, Wolff E (2003) Recent rapid regional climate warming on the Antarctic Peninsula. Clim Change 60:243–274

Velázquez D, Rochera C, Camacho A, Quesada A (2011) Temperature effects on carbon and nitrogen metabolism in some maritime Antarctic freshwater phototrophic communities. Polar Biol 34:1045–1055

Vincent WF, Howard-Williams C (1986) Antarctic stream ecosystem: physiological ecology of a blue-green algal epilithon. Freshw Biol 16:219–233

Vincent WF, Howard-Williams C, Broady PA (1993) Microbial communities and processes in Antarctic flowing waters. In: Friedman EI (ed) Antarctic microbiology. Wiley, New York, pp 543–569